

**EVOLUTION OF FLUID COMPOSITION INFERRED FROM CALCITE IN THE YAMAOTO 791198 CM CHONDRITE.** W. Fujiya<sup>1</sup>, Y. Aoki<sup>1</sup>, T. Ushikubo<sup>2</sup>, and K. Hashizume<sup>1</sup>, <sup>1</sup>Faculty of Science, Ibaraki University, 2-1-1 Bunkyo, Mito, Ibaraki 310-8512, Japan (wataru.fujiya.sci@vc.ibaraki.ac.jp), <sup>2</sup>Kochi Institute for Core Sample Research, JAMSTEC, 200 Monobe-otsu, Nankoku, Kochi 783-8502, Japan.

**Introduction:** Carbonate minerals are the second major C-bearing component and are ubiquitous in CM chondrites [1]. They formed by aqueous alteration in the CM chondrite parent body [2,3]. Previous studies have revealed a large variation in C isotope ratios of CM carbonates with  $\delta^{13}\text{C}$  values ranging from  $\sim 20$  to  $\sim 90$  ‰ [e.g., 4-11]. However, the reason for this variability has remained poorly understood. This is because physicochemical conditions of aqueous alteration were likely diverse even within a single meteorite specimen [7], which makes it difficult to trace the change in  $\delta^{13}\text{C}$  values of carbonates by comparing  $\delta^{13}\text{C}$  values of different carbonate grains or bulk meteorite samples.

To overcome this problem, here we studied carbonate grains with similar textures suggesting a common genetic origin, and conducted *in-situ* C- and O-isotope measurements by Secondary Ion Mass Spectrometry (SIMS) on multiple spots within single carbonate grains. We measured C and O isotope ratios along the crystal growth of carbonate grains, which was inferred from spatial distribution of minor element abundances and cathodoluminescence (CL) intensity.

**Experimental:** We searched for carbonate grains in a polished thin section of Yamato 791198 (CM 2.4) using an SEM (JEOL JSM-5600LV) at Ibaraki University. Prior to the isotope analyses, we obtained CL images of seven calcite ( $\text{CaCO}_3$ ) grains with an FE-EPMA (JEOL JXA-8530F) at University of Tokyo. To avoid a possible damage by electron beam bombardment, we limited the beam current to  $\sim 5$  nA. Then, we measured O isotope ratios of the calcite grains with the CAMECA ims-1280 at Kochi Institute for Core Sample Research, JAMSTEC. Negative ions of  $^{16}\text{O}^-$ ,  $^{17}\text{O}^-$ , and  $^{18}\text{O}^-$ , produced by a focused  $\text{Cs}^+$  primary ion beam ( $\sim 30$  pA, 3-4  $\mu\text{m}$  in diameter), were simultaneously detected with a Faraday cup (FC) and two electron multipliers (EMs). The typical uncertainties on  $\delta^{17}\text{O}$ ,  $\delta^{18}\text{O}$ , and  $\Delta^{17}\text{O}$  values were  $\sim 1.7$  ‰,  $\sim 1.1$  ‰, and  $\sim 0.7$  ‰ ( $2\sigma$ ), respectively. Typically, the measurements were carried out on three different points for each calcite grain. After the O-isotope measurement, the thin section was slightly polished. Next, we measured C isotope ratios of the calcite grains with the same instrument as that for the O-isotope measurement. Negative ions of  $^{12}\text{C}^-$ ,  $^{13}\text{C}^-$ , and  $^{13}\text{C}^1\text{H}^-$ , produced by a focused  $\text{Cs}^+$  primary ion beam ( $\sim 120$  pA, 6-8  $\mu\text{m}$  in diameter), were simultaneously detected with a Faraday cup (FC)

and two electron multipliers (EMs). The uncertainty on  $\delta^{13}\text{C}$  values was typically  $\sim 1.1$  ‰ ( $2\sigma$ ). The measurements were performed just upon the points where the O isotope ratios were measured (if possible), or adjacent regions to those for the O-isotope measurements. Finally, we obtained quantitative chemical compositions and elemental maps of Mg, Si, Ca, Mn, and Fe of the calcite grains using the same FE-EPMA as that for the CL images with a beam current of  $\sim 30$  nA.

**Results and discussion:** A backscattered electron image (BEI), color CL image, and Mn distribution of a representative calcite grain are shown in Fig. 1.

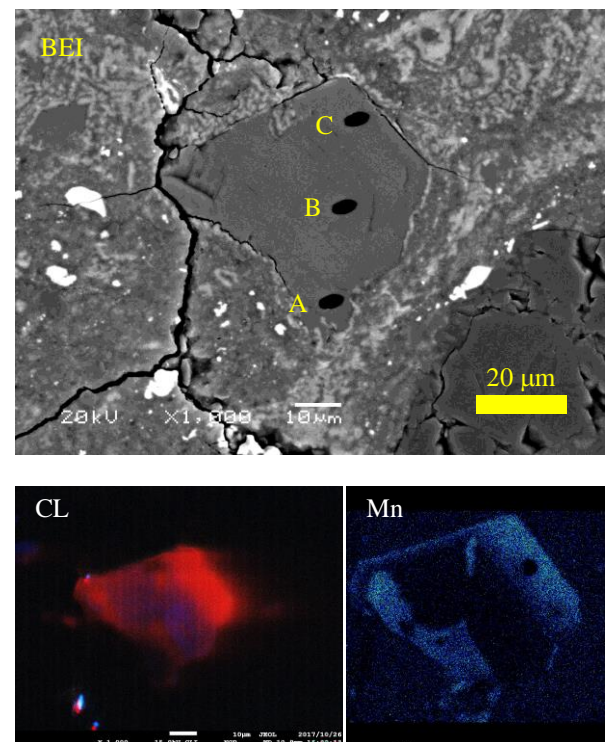


**Fig. 1:** BEI (top), color CL (lower left), and Mn distribution (lower right) of a calcite grain in Y791198. Black ovals in the BEI are the SIMS analytical spots.

This grain exhibits a clear zoning of Mn (also Mg and Fe, not shown here). This zoning is well correlated with the CL image. The heterogeneous distribution of minor elements and CL intensity likely reflects the crystal growth of this grains. This grain has clear crystal facets on the upper edge while the shape of the lower edge is irregular. Thus, this subhedral grain seems to

have grown in a fluid-filled pore space from an irregular-shaped pore margin.

The O isotope ratios of the calcite grains significantly vary with the  $\delta^{18}\text{O}$  values ranging from  $\sim 22$  to  $\sim 38$  ‰ (Fig. 2). The O isotope ratios plot on a single trend line in an O three-isotope plot with a slope of  $\sim 0.61$ , slightly steeper than the terrestrial fractionation line, reflecting a progressive O-isotope exchange between initially  $^{16}\text{O}$ -poor water and  $^{16}\text{O}$ -rich rock [12,13]. This is also the case within individual grains: the grain in Fig. 1 has variable  $\delta^{18}\text{O}$  values of  $\sim 37$  ‰ (A),  $\sim 27$  ‰ (B), and  $\sim 25$  ‰ (C), which correspond to the analytical spots shown in Fig. 1. This  $\delta^{18}\text{O}$  change demonstrates that the crystal grew from a relatively dark CL core (A) to a red CL periphery (C). This inferred crystal growth is consistent with the morphology of this grain. Interestingly, Mg, Mn, and Fe abundances do not increase monotonically with the crystal growth. The blue CL mantle has low MnO and MgO contents ( $\sim 0.07$  wt% and  $\sim 0.06$  wt%, respectively) relative to the dark CL core and the red CL periphery (0.50-0.97 wt% and 0.29-0.90 wt%, respectively). The dark CL in the core likely results from an FeO enrichment ( $\sim 2.01$  wt%). These observations along with the clear boundary of the CL image and minor element distribution suggest that the crystal grew intermittently, for which alteration of various mineral phases (e.g., Ca-rich glass, Fe-Ni metal, plagioclase, and mafic silicate) with different reaction rates may be responsible.

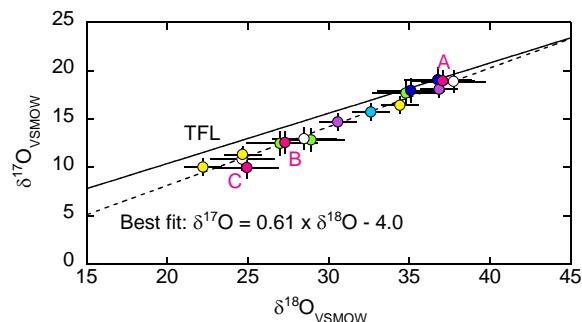


**Fig. 2:** Oxygen isotope ratios of calcite grains in Y791198. Analyses on the same grain are represented by the same color. Data points A, B, and C correspond to the SIMS analytical spots shown in Fig. 1.

The  $\delta^{13}\text{C}$  values of the calcite grains range from 17 to 32 ‰ (Fig. 3). This range is much smaller than that observed for different carbonate grains or bulk meteorite samples by previous studies. Especially, the  $\delta^{13}\text{C}$  variations within individual grains are only 4 ‰ at most except for one grain. Previous studies have suggested that the observed  $\delta^{13}\text{C}$  variation was produced by the Rayleigh-type isotopic fractionation by the es-

cape of  $^{13}\text{C}$ -poor methane [5], or equilibrium isotopic fractionation reflecting variable formation temperatures of carbonates [6]. However, the small intra-grain  $\delta^{13}\text{C}$  variations associated with the large  $\delta^{18}\text{O}$  change observed in this study cannot be explained by such processes. Instead, here we propose that the  $\delta^{13}\text{C}$  values of dissolved carbon species in aqueous solutions were locally heterogeneous, and did not significantly change during carbonate formation. Fujiya et al. suggested that the variable  $\delta^{13}\text{C}$  values of CM carbonates are attributed to the mixing between two carbon reservoirs with different C isotope ratios, namely,  $^{13}\text{C}$ -rich  $\text{CO}_2$  ice and  $^{13}\text{C}$ -poor organic matter, with variable proportions [10]. Our new data are more consistent with this argument.

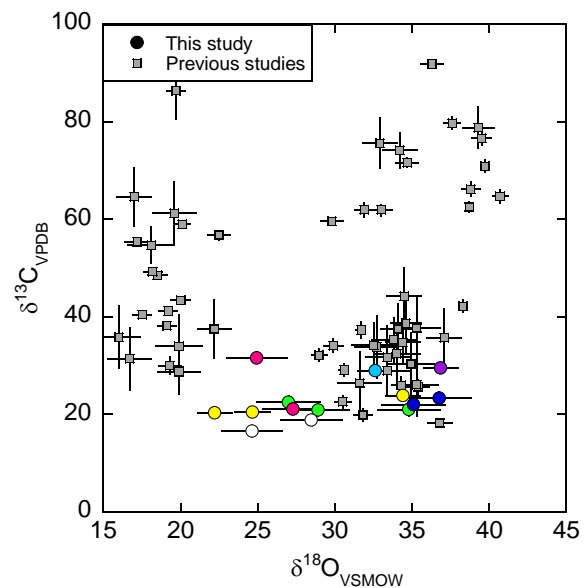


**Fig. 3:**  $\delta^{13}\text{C}$  vs.  $\delta^{18}\text{O}$  values of calcite grains in Y791198. Colors are as in Fig. 2. Previous data [7-10] are shown by gray (*in-situ* SIMS analyses of Ca-carbonates only).

**References:** [1] Smith J. W. and Kaplan I. R. (1970) *Science*, 167, 1367-1370. [2] Brearley A. J. (2006) in *Meteorites and the Early Solar System II*, 587-624. [3] Lee M. R. et al. (2014) *GCA*, 144, 126-156. [4] Grady M. M. et al. (1988) *GCA*, 52, 2855-2866. [5] Guo W. and Eiler J. M. (2007) *GCA*, 71, 5565-5575. [6] Alexander C. M. O'D. et al. (2015) *Meteoritics & Planet. Sci.*, 50, 810-833. [7] Fujiya W. et al. (2015) *GCA*, 161, 101-117. [8] Vacher L. G. et al. (2017) *GCA*, 213, 271-290. [9] Vacher L. G. et al. (2018) *GCA*, 239, 213-234. [10] Fujiya W. et al. (2018) *LPS XLIX*, Abstract #1377. [11] Tyra M. et al. (2016) *GCA*, 175, 195-207. [12] Clayton R. N. and Mayeda T. K. (1984) *EPSL*, 67, 151-161. [13] Fujiya W. (2018) *EPSL*, 481, 264-272.